esa

ECOSPHERE

Estimating animal densities in the aerosphere using weather radar: To Z or not to Z?

PHILLIP B. CHILSON,[1,2,]† WINIFRED F. FRICK,[3] PHILLIP M. STEPANIAN,[1,2] J. RYAN SHIPLEY,[4] THOMAS H. KUNZ,[5] AND JEFFREY F. KELLY[6,7]

[1]*School of Meteorology, University of Oklahoma, Norman, Oklahoma 73072 USA*
[2]*Advanced Radar Research Center, University of Oklahoma, Norman, Oklahoma 73072 USA*
[3]*Department of Ecology and Evolutionary Biology, University of California, Santa Cruz, California 95064 USA*
[4]*Center for Spatial Analysis, University of Oklahoma, Norman, Oklahoma 73072 USA*
[5]*Center for Ecology and Conservation Biology, Boston University, Boston, Massachusetts 02215 USA*
[6]*Oklahoma Biological Survey, University of Oklahoma, Norman, Oklahoma 73019 USA*
[7]*Department of Biology, University of Oklahoma, Norman, Oklahoma 73072 USA*

Citation: Chilson, P. B., W. F. Frick, P. M. Stepanian, J. R. Shipley, T. H. Kunz, and J. F. Kelly. 2012. Estimating animal densities in the aerosphere using weather radar: To Z or not to Z? Ecosphere 3(8):72. http://dx.doi.org/10.1890/ES12-00027.1

Abstract. Weather radars provide near-continuous recording and extensive spatial coverage, which is a valuable resource for biologists, who wish to observe and study animal movements in the aerosphere over a wide range of temporal and spatial scales. Powerful biological inferences can be garnered from radar data that have been processed primarily with the intention of understanding meteorology. However, when seeking to answer certain quantitative biological questions, e.g., those related to density of animals, assumptions made in processing radar data for meteorological purposes interfere with biological inference. In particular, values of the radar reflectivity factor (Z) reported by weather radars are not well suited for biological interpretation. The mathematical framework we present here allows researchers to interpret weather radar data originating from biological scatterers (bioscatterers) without relying on assumptions developed specifically for meteorological phenomena. The mathematical principles discussed are used to interpret received echo power as it relates to bioscatterers. We examine the relationships among measurement error and these bioscatter signals using a radar simulator. Our simulation results demonstrate that within 30–90 km from a radar, distances typical for observing aerial vertebrates such as birds and bats, measurement error associated with number densities of animals within the radar sampling volume are low enough to allow reasonable estimates of aerial densities for population monitoring. The framework presented for using radar echoes for quantifying biological populations observed by radar in their aerosphere habitats enhances use of radar remote-sensing for long-term population monitoring as well as a host of other ecological applications, such as studies on phenology, movement, and aerial behaviors.

Key words: radar; aeroecology; bioscatter; phenology.

Received 2 February 2012; revised 4 May 2012; accepted 24 May 2012; final version received 11 July 2012; **published** 16 August 2012. Corresponding Editor: D. P. C. Peters.

† **E-mail:** chilson@ou.edu

Introduction

There is a long tradition of incorporating radar technology into biological studies as a means of observing movements of airborne animals and quantifying their numbers in the lower atmosphere (Gauthreaux 2006). Much of this research has been conducted using radar systems that have been specifically adapted for observations of volant species (e.g., Bruderer et al. 1999, Harmata et al. 2003, Chapman et al. 2011, Alerstam et al. 2011). However, some investigators have chosen to incorporate data from operational radar systems (those designed for routine operation) into their biological studies. One example is the use of weather radar, such as those deployed by national weather services, to study birds, bats, and insects (Gauthreaux et al. 2008, van Gasteren et al. 2008, Dokter et al. 2011, Chilson et al. 2012, Kelly et al. 2012). Indeed, Gauthreaux (1970) began using weather radars in the US for biological research not long after these facilities were established in 1959. Radar technology has greatly advanced since that time, and it has become increasingly easier to access and process weather radar data with the advent of faster processing and data storage capabilities. Consequently, we are witnessing a rapidly growing interest in integrating radar data into biological studies.

Weather radars are designed to provide continuous observations over extended spatial domains. Often several weather radar stations are networked together to further extend the spatial coverage. For example, the US National Weather Service operates over 150 weather surveillance Doppler radars (WSR-88D) with the majority of these located in the continental US (Crum et al. 1998, Serafin and Wilson 2000, Kelleher et al. 2007). Collectively the network of radars is known as NEXt generation RADar (NEXRAD) and data from this network are freely available from the National Climate Data Center (NCDC) via the Internet. As such, researchers can readily request radar observations and incorporate them into their studies of animal behavior in the aerosphere (lower atmosphere) over a wide range of spatial and temporal scales (Chilson et al. 2012). Researchers now have access to a wealth of data through numerous archives: meteorological, climatological, topographical, land cover, land usage, and others. The effective utilization of these data requires the integration of atmospheric science, earth science, geography, ecology, computer science, computational biology, and engineering. This transdisciplinary approach to further understanding of biological patterns and processes in the aerosphere is known as aeroecology (Kunz et al. 2008).

As with any cross-disciplinary research enterprise, to effectively utilize the technology and understanding offered by other subject areas, one must become familiar with their particular parlance and terminology. This is certainly true when integrating weather radar data into aeroecology. To make optimal use of weather radar data for biological studies, it is important to understand how radio waves interact with biological scatterers (bioscatterers) in the aerosphere. For inferential studies of animal behavior and movements, it is sufficient to be able to discriminate bioscatter from weather signals and then use the bioscatter to track the presence and movements of animals (Horn and Kunz 2008, Buler and Moore 2011, Kelly et al. 2012). However, if the goal of a study is to quantify the number of animals in the aerosphere (Russell and Gauthreaux 1998, Gauthreaux 1970, Liechti et al. 1995, Gauthreaux and Belser 1998, Diehl et al. 2003, Nebuloni et al. 2008) then a more fundamental understanding of bioscatter is required.

The intensity of backscattered signals reported by weather radars is typically given in terms of a *radar reflectivity factor*. The radar reflectivity factor has been specifically devised to facilitate interpretation of radar echoes received from precipitation. Moreover, calculation of the radar reflectivity factor relies on several simplifying assumptions. When dealing with radio wave scatter from biological entities (bioscatter), however, a more meaningful and intuitive measure of echo power is *radar reflectivity*. Under the appropriate conditions, radar reflectivity can be directly related to the number of animals present within a sampled volume of space. Fortunately, reported values of the radar reflectivity factor from weather radars can be readily converted to radar reflectivity.

Our purpose is to describe mathematical relationships between bioscatterers and radar

reflectivity based on conventional weather radar properties and to illustrate how this remote sensing capability can be used when observing and measuring biological entities in the aerosphere. We (1) discuss the relationship between the radar reflectivity factor and radar reflectivity, (2) highlight some of the assumptions involved when calculating these two parameters, (3) demonstrate why the radar reflectivity factor is not well suited for biological studies, and (4) explain how to calculate radar reflectivity from the radar reflectivity factor. We then use results from a Monte-Carlo based radar simulation to demonstrate how much variance one should expect when estimating radar reflectivity from bioscatter under various conditions.

Increased access to archived weather radar products has sparked interest in various biological uses of radar data (e.g., Russell and Gauthreaux 1998, Gauthreaux and Belser 1998, Diehl et al. 2003, Horn and Kunz 2008, Buler and Diehl 2009, Dokter et al. 2011, Chilson et al. 2012, Kelly et al. 2012). Advanced investigations that use these remotely sensed data to quantify population densities of animals in the aerosphere require a rigorous understanding of the basic mathematical properties and inherent assumptions in analyzing radar echo power. Several radar tutorials for biologists already exist (e.g., Bruderer 1997*a*, *b*, Gauthreaux and Belser 2003, Diehl and Larkin 2005, Larkin and Diehl 2012) and much of the mathematical content provided below in the Background Section can be found in various papers and books that deal with radar hardware, radar signal processing, or the interpretation of weather radar signals (Battan 1973, Sauvageot 1992, Doviak and Zrnić 1993, Rinehart 2004). To clarify the mathematical properties of radar data and demonstrate their utility for ecological investigations, we extract and synthesize those components most germane for analyzing bioscatter.

Background

Simplified radar equation

To demonstrate the importance of the distinctions between radar reflectivity and the radar reflectivity factor and their relationships to bioscatter, we examine the basic radar equation, which is used to calculate the power of the backscattered electromagnetic radiation received by a radar. Radars transmit electromagnetic radiation in the form of radio waves through the use of an antenna. The transmitted radiation interacts with an object or objects and the scattered energy is received by either the same antenna used for transmission (monostatic) or a separate antenna (bistatic). The expected power of the received radiation is calculated using the basic radar equation. For the case of scatter from a single object located at a distance r (m) from a monostatic radar, the received power P_r (W) is given by a simplified form of the radar equation:

$$P_r = P_t \frac{G^2 \lambda^2 \sigma}{64\pi^3 r^4} \quad (1)$$

where P_t (W) is the transmit power of the radar, G is the gain of the antenna, λ (m) is the wavelength of the radio waves, and σ (m^2) is the radar cross section (RCS) of the scatterer (Rinehart 2004). Antenna gain is basically a measure of an antenna's capacity to amplify signal power (sensitivity) as a function of orientation and can be related to the radar wavelength and the effective area of the antenna. The RCS of an object is a measure of how reflective it is to radio waves of a given wavelength and has units of area. RCS values can be different than the physical area of the object intercepting radio waves. The value of σ generally is a function of the scattering angle with respect to incident angle and since all operational weather radars are monostatic, the scattering angle is oriented in the opposite direction of the incident angle for backscatter.

In the treatment that follows, we consider two variants of the radar equation based on the underlying density and distribution of the animals sampled by the radar. In the first case, which we call *discrete bioscatter*, it is assumed that the received power P_r can be attributed to scatter from individual animals. We refer to the second case as *distributed bioscatter*. Here we assume that the sampled animals are uniformly distributed in space and that they are sufficiently abundant to be treated as a "continuum" of scatterers. These cases are not unique to bioscatter. It is common to consider discrete and distributed scatter when using radar to study geophysical phenomena such as precipitation and ionized media (plasma) (Doviak and Zrnić 1993). A thorough under-

standing of the differences between discrete and distributed bioscatter is needed when attempting to quantify animal densities in the aerosphere using radar. Although the focus of the following discussion is predominantly on weather radar, the treatment applies to most radars used for biological studies.

Radar equation for discrete bioscatter

The radar equation given by Eq. 1 is fundamentally correct; however, it does not explicitly account for certain sensitivity effects introduced by the radar, such as those attributed to range and beam weighting as described below. For the case of weather radar, the gain of the antenna (and therefore its sensitivity) is greatest along the radial component corresponding to the antenna pointing direction and decreases as a function of angle measured relative to that radial; ignoring the effects of antenna side lobes, which is beyond the scope of our discussion here. That is, the contribution of a scatterer to the total received power is weighted according to its angular location taken with respect to the pointing direction of the antenna. The so-called one-way beam weighting function can be expressed approximately as

$$f^2(\theta,\phi) = \exp\left(-\frac{\theta^2}{2\sigma_\theta^2} - \frac{\phi^2}{2\sigma_\phi^2}\right) \qquad (2)$$

where θ and ϕ are angles oriented along the horizontal and vertical plane of the transmitted radio wave, respectively. These angles are measured with respect to the antenna pointing direction (θ_o, ϕ_o) (Probert-Jones 1962). Furthermore, $\sigma_\theta = \theta_1/\sqrt{2\ln 2}$ and $\sigma_\phi = \phi_1/\sqrt{2\ln 2}$ with θ_1 and ϕ_1 being the one-way half-power (3 dB) beamwidths in the horizontal and vertical planes, respectively. The half-power beamwidths are only reference points; however, they are often used when discussing the extent of a radar sampling volume transverse to the beam direction.

Weather radars do not transmit radio waves continuously, but rather send out pulses of energy as a means of determining the range of detected scatterers. Since the propagation speed of radio waves in the atmosphere is known, range can be determined from the measured time delay between pulse transmission and reception of the scattered energy. We refer to this distance as r_o. Owing to hardware constraints and limitations in frequency allocation, radars must operate within finite bandwidths (frequency bounds), which dictate the minimum pulse duration allowed. Furthermore, best performance of the radar can be achieved when the receiver's filter is matched to the transmit pulse (Doviak and Zrnić 1993). A matched filter is designed to maximize a radar's signal-to-noise ratio. For a pulsed radar of a given bandwidth and corresponding matched filter, a simplified form of the one-way range weighting function can be written approximately as

$$W(r) = \exp\left[-\frac{(r-r_o)^2}{4\sigma_r^2}\right] \qquad (3)$$

(Doviak and Zrnić 1984). Here r is the magnitude of the vector directed from the radar antenna to a region of space being probed by the radar, $\sigma_r = 0.35\ \Delta r$, and $\Delta r = c\tau/2$, with c being the speed at which the electromagnetic radiation propagates through the atmosphere (approximately equal to the speed of light in a vacuum) and τ is the duration of the transmitted wave. The quantity Δr is often referred to as the range resolution. Note that $W(r)$ attains its maximum value at r_o.

The backscattered power resulting from a single bioscatterer having an RCS of σ and location given by (r, θ, ϕ) with respect to the radar antenna is given by

$$P_r = P_t \frac{G^2\lambda^2}{64\pi^3 r^4} W^2(r) f^4(\theta,\phi)\sigma. \qquad (4)$$

Therefore, the power received by a radar for a single discrete bioscatterer (e.g., individual animal) depends on its RCS value, range from the antenna, and angular location with respect to the pointing direction of the antenna. In the most general case, σ also exhibits an angular dependence, which we are not explicitly considering here. Although we are able to determine r_o and the pointing direction of the antenna (θ_o, ϕ_o), the precise location of the bioscatter within the sampling volume cannot be retrieved. The degree of uncertainty in determining the bioscatterer's location is prescribed by $W^2(r)$ and $f^4(\theta, \phi)$.

Typically, the bioscatter received by weather radars is not attributed to a single animal but rather a collection of animals. If we consider the

backscattered power for a collection of scatterers (e.g., group of animals aloft) then the received power becomes

$$P_r = P_t \frac{G^2 \lambda^2}{64\pi^3} \sum_i W^2(r_i) f^4(\theta_i, \phi_i) \frac{\sigma_i}{r_i^4} \qquad (5)$$

where the summation includes all bioscatterers. Although the summation is taken, in principle, over all bioscatterers, only those in the vicinity of (r_o, θ_o, ϕ_o) will contribute appreciably to the received power. As for the case involving a single bioscatterer, we cannot resolve the actual locations of the individuals nor their corresponding contributions to the total received power.

Radar equation for distributed bioscatter

If the bioscatterers are uniformly distributed in space within the region being probed by the radar and the number of scatterers under consideration is sufficiently large then we can simplify Eq. 5 by introducing the concept of a radar sampling volume. Clearly a radar pulse transmitted by an antenna will only effectively illuminate a finite region of space. A radar sampling volume produced by the beam and range weighting functions given by Eq. 2 and Eq. 3, respectively, can be expressed as

$$V_{rad} = r_o^2 \int_r W^2(r) dr \int_\Omega f^4(\theta, \phi) d\Omega \qquad (6)$$

where Ω is the solid angle subtended by the center of the sampling volume. As the number of bioscatterers being observed becomes large, we can assume that they are uniformly distributed throughout the sampling volume and therefore treat the summation of discrete entities as an integral over a continuum of volume scatter multiplied by the number density of the entities weighted by their individual RCS values and their ranges. This is referred to as the *volume-filling assumption*. In this case

$$\sum_i W^2(r_i) f^4(\theta_i, \phi_i) \frac{\sigma_i}{r_i^4} \rightarrow \left[\frac{1}{\Delta V} \sum_{vol} \frac{\sigma_i}{r_o^4} \right] V_{rad} \qquad (7)$$

where $\sum_{vol}$ represents the summation over all scatterers within a unit volume ΔV and we have used $r_i \approx r_o$. That is, the total number of scatterers being considered is the number of scatterers contained within a unit volume times the radar sampling volume given by Eq. 6. The effect of the weighting functions are accounted for by our definition of the radar sampling volume.

The next task is to express Eq. 6 in an analytic form. It was shown by Probert-Jones (1962) that

$$r_o^2 \int_\Omega f^4(\theta, \phi) d\Omega \approx \frac{\pi r_o^2 \theta_1 \phi_1}{8 \ln(2)} \qquad (8)$$

and it can easily be shown that

$$\int_r W^2(r) dr = \sqrt{2\pi} 0.35 \Delta r. \qquad (9)$$

Therefore, the radar sampling volume is given by

$$V_{rad} = \frac{0.35\sqrt{2\pi}}{2\ln 2} \left(\frac{\pi r_o^2 \theta_1 \phi_1 \Delta r}{4} \right) \qquad (10)$$

where the quantity in parenthesis is equivalent to truncated oval-based cone having diameters along the horizontal and vertical axes of $r_o\theta_1$ and $r_o\phi_1$, respectively and a length of Δr. This is depicted in Fig. 1. We should note that the factor of $\sqrt{2\pi}0.35$ resulting from the range weighting function shown in Eq. 10 is sometimes included into the radar equation as a loss factor caused by having a finite receiver bandwidth (Doviak and Zrnić 1993).

As shown in Eq. 10, the radar sampling volume increases with range. Consider a collection of bioscatterers uniformly distributed in space or at least uniformly distributed within a localized region of interest. In this case we can define a bioscatter number density N_{bio} as the number of bioscatterers per unit volume. Then the *effective* number of bioscatterers contributing to the receiver power in the radar equation is simply $V_{rad} \cdot N_{bio}$. In the next section we discuss how a non-uniform distribution of bioscatterers can be treated.

Radar reflectivity and radar reflectivity factor

The cumulative backscattering cross section per unit volume is referred to as the radar reflectivity or sometimes simply the reflectivity η. The value of η is defined as

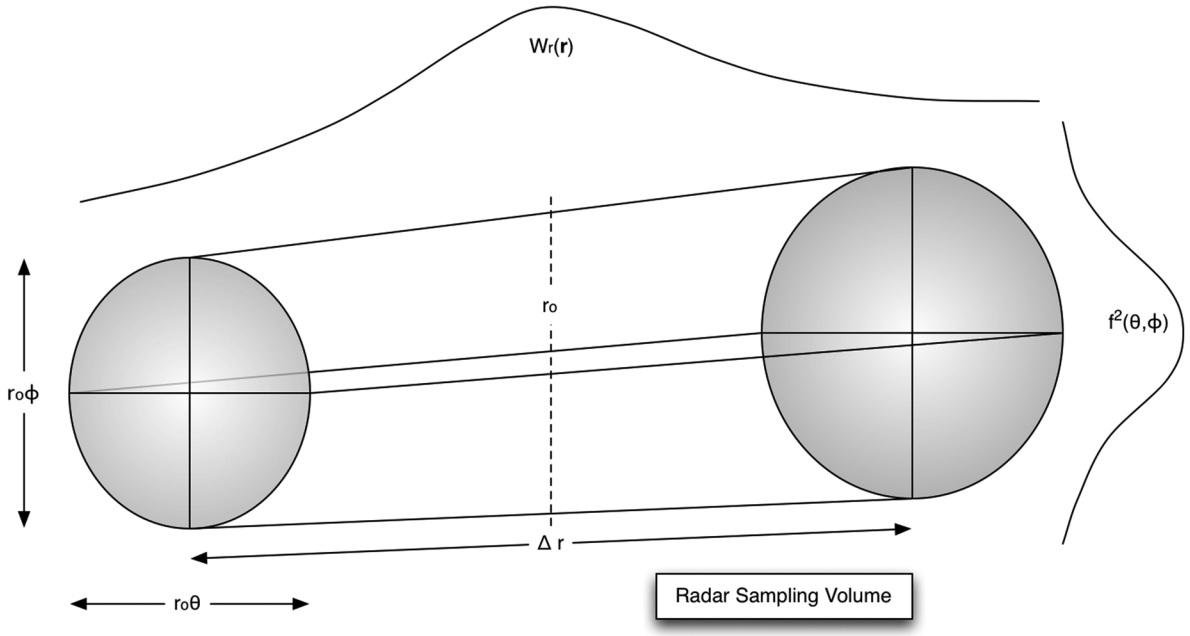

Fig. 1. Illustration depicting the radar sampling volume discussed in the text. The one- way range and beam weighting functions are represented by $f^2(\theta, \phi)$ and $W(r)$, respectively.

$$\eta \equiv \frac{1}{\Delta V}\sum_{\text{vol}} \sigma_i \tag{11}$$

(Doviak and Zrnić 1993, Rinehart 2004). Combining the equations discussed above we finally arrive at a form of the radar equation useful for biological applications

$$\eta = \frac{64\pi^3 r_o^4}{G^2\lambda^2 V_{\text{rad}}}\frac{P_r}{P_t} = \frac{512(\ln 2)\pi^2 r_o^2}{0.35\sqrt{2\pi}G^2\lambda^2\theta_1\phi_1\Delta r}\frac{P_r}{P_t}. \tag{12}$$

This equation assumes a large number of bioscatterers uniformly distributed within the radar sampling volume. If the bioscatter can be described through a number density N_{bio} with each animal having an RCS of σ then the radar reflectivity simply becomes

$$\eta = \frac{1}{\Delta V}\sum_{\text{vol}} \sigma = N_{\text{bio}}\sigma. \tag{13}$$

Therefore, under these conditions, it is possible to calculate N_{bio} directly from the radar estimate of η.

The magnitude of the backscattered signal for weather radars is not reported directly as radar reflectivity but rather as a radar reflectivity factor. Whereas radar reflectivity naturally lends itself to applications involving the quantitative analysis of bioscatter, this is not the case for the radar reflectivity factor. The radar reflectivity factor has been specifically developed for the study of precipitation and as such, contains many assumptions that are customized for this application, but could inhibit biological interpretability of radar signals.

In the beginning of the 20th century, Gustav Mie formulated a rigorous theory (Mie scattering theory) to describe the scatter of electromagnetic waves by suspended particles (Mie 1908). To create a tractable theoretical framework, he assumed the particles to be spherical and composed of a dielectric material having a complex permittivity (Mie 1908). If you assume that the diameter of the particle D is small compared to the wavelength of the electromagnetic wave, e.g., $D \leq \lambda/16$ (Doviak and Zrnić 1993), then

$$\sigma = \frac{\pi^5}{\lambda^4}|K_m|^2 D^6 \tag{14}$$

where $K_m = (m^2 - 1)/(m^2 + 2)$ and $m = n + i\kappa$ is the complex refractive index of the material. Here, n

is the conventional refractive index related to the phase speed of waves in a dielectric medium compared to its speed in a vacuum and κ is the absorption coefficient (Battan 1973, Doviak and Zrnić 1993). The condition described by Eq. 14 is known as the Rayleigh approximation and represents a special case of the full Mie scattering theory. For weather radars, the Rayleigh approximation can typically be applied for precipitation particles and in this case

$$\eta = \frac{\pi^5}{\lambda^4}|K_m|^2 Z \tag{15}$$

where the radar reflectivity factor Z is defined as

$$Z \equiv \frac{1}{\Delta V}\sum_{\text{vol}} D_i^6. \tag{16}$$

For the case of precipitation, we can further assume that the dielectric material of the scatterers is water; however, the actual value that we assign to m depends on the water's phase and temperature and the wavelength of the radar. Since these properties of the water are not in general known, values of the radar reflectivity factor reported by weather radars are given as the *equivalent* radar reflectivity factor Z_e defined as

$$Z_e = \frac{\lambda^4}{\pi^5|K_m|^2}\eta \tag{17}$$

where η is obtained from Eq. 12. Here, we not only assume that the Rayleigh approximation holds but also that all scatterers consist of liquid water, resulting in $|K_m|^2 = 0.93$, which is valid for wavelengths used by most weather radars. That is, the equivalent radar reflectivity value represents the value that would be associated with the observed backscatter if it were attributed to volume-filling liquid precipitation in the Rayleigh regime.

Because the radar reflectivity factor Z (or equivalent radar reflectivity Z_e) can have such a wide dynamic range, values are commonly reported and discussed using a logarithmic scale

$$Z[\text{dBZ}] = 10\log_{10}\left(\frac{Z}{1\ \text{mm}^6/\text{m}^3}\right). \tag{18}$$

Values of Z_e for meteorological phenomena might range from about 10–20 dBZ for light rain to 60–70 dBZ for severe weather events involving hail. As we can see, the assumptions used to derive values of radar reflectivity factor have little relevance for quantitative studies of bioscatter.

Reflectivity as a biological parameter

Unlike the radar reflectivity factor Z, radar reflectivity η is a quantity that can be directly related to bioscatter. The units of η are inverse length, e.g., 1/m since we are dealing with the total effective scattering area per unit volume. There are far fewer assumptions associated with radar reflectivity as compared to the radar reflectivity factor. Fortunately, we can readily convert values of Z_e to η if we know the wavelength of the radar that was used to make the measurements.

Consider as an example an equivalent radar reflectivity factor of 15 dBZ reported for NEXRAD. From Eq. 18 we see that 15 dBZ corresponds to a value of 32 mm^6/m^3 (or equivalently 32×10^{-18} m^3) in linear units. NEXRAD operates at a wavelength of $\lambda = 0.107$ m. Therefore, using Eq. 17 we find that $Z_e = 15$ dBZ translates to $\eta = 6.9 \times 10^{-11}$/m. A more meaningful biological interpretation of η results if we express this quantity in units of square centimeters per cubic kilometer (cm^2/km^3), a convention already used by some (e.g., Dokter et al. 2011, Shamoun-Baranes et al. 2011). That is, a value of $Z_e = 15$ dBZ as measured using NEXRAD corresponds to $\eta = 690$ cm^2/km^3. A value of 690 cm^2/km^3 could be produced, for example, by about 86 willow warblers per cubic kilometer (9 g and $\sigma = 8$ cm^2) or 345 song thrushes per cubic kilometer (70 g and $\sigma = 2$ cm^2) or 17 woodpigeons per cubic kilometer (500 g and $\sigma = 40$ cm^2), where the mass and RCS values are taken from (Alerstam 1990). These RCS values were calculated using Mie scattering theory for equivalent-mass spheres of water. That is, the scattering properties of an animal are assumed to be equivalent to those of a sphere of water having the same mass as the animal (Eastwood 1967). Note that the RCS values given in the example do not increase monotonically with mass or size. This is because the sizes of the equivalent-mass spheres fall within the resonant regime of the Mie scattering theory for NEXRAD (Martin and Shapiro 2007). We should also note that Mie theory does not account for the shape or orientation of a scatterer,

since a spherical dielectric is assumed.

Just as 1 mm^6/m^3 is used as a reference value when reporting radar reflectivity factor, we could use 1 cm^2/km^3 as a reference value for η and then plot or discuss reflectivity for bioscatter in logarithmic units. That is, our η of 690 cm^2/km^3 would be 28 dB (calculated using $10\log_{10}(\eta/\eta_0)$), where $\eta_0 = 1$ cm^2/km^3. For a given wavelength, it then becomes easy to convert from a radar reflectivity factor in dBZ to radar reflectivity in dB using

$$\eta[\mathrm{dB}] = Z[\mathrm{dBZ}] + \beta \tag{19}$$

where $\beta = 10\log_{10}(10^3\pi^5|K_m|^2/\lambda^4)$ with λ expressed in cm and $|K_m|^2 = 0.93$ and the factor of 10^3 is needed to account for unit conversion. For example, $\beta = 14.54$ for $\lambda = 10$ cm (S-band), $\beta = 26.58$ for $\lambda = 5$ cm (C-band), and $\beta = 35.46$ for $\lambda = 3$ cm (X-band), which are common values for weather radars. When using Eq. 19, one should ideally use the exact wavelength of the radar, since the calculation of β is sensitive to the value of λ.

When calculating the radar reflectivity factor from radar reflectivity, it is assumed that the volume-filling assumption applies. If this is not the case, then η calculated using Eq. 12 must be interpreted as the weighted sum of bioscatterers within the radar sampling volume normalized by the radar sampling volume:

$$\eta \rightarrow \frac{1}{V_{\mathrm{rad}}} \sum_i W^2(r_i) f^4(\theta_i, \phi_i) \sigma_i. \tag{20}$$

As we discussed earlier, under these conditions there is no means of knowing the locations of the bioscatterers within radar sampling volume or their corresponding weights, which results in some inherent patterns in the variance around the estimate η even if σ and N_{bio} are constant. To quantify this relationship we present a Monte-Carlo simulation study of these patterns in variation and interpret the results relative to our ability to quantify the density of bioscatterers in the aerosphere.

Methods

Radar simulator for bioscatterers

If the radar is sampling a sufficiently large number of bioscatterers, then the volume-filling assumption allows us to simply relate the bioscatter to the product of a number density and radar sampling volume. Although the volume-filling assumption greatly simplifies the radar equation and makes it possible to quantitatively utilize bioscatter observations, the question arises: what is sufficiently large? Moreover, what are the consequences of assuming volume-filling even though the number of sampled bioscatterers is not sufficiently large or not uniformly distributed?

To address these questions we developed a simple radar simulator to assess uncertainties in estimating radar reflectivity from bioscatter. The simulator is written in MATLAB and utilizes a Monte Carlo simulation approach (Eckhardt 1987) to account for variability in the locations of bioscatterers. The primary scattering routine in the simulator calculates backscattered power P_r, radar reflectivity η, and effective radar reflectivity factor Z_e for an assumed radar configuration and specified values of the range r_o, bioscatter number density N_{bio}, and radar cross section σ. This routine operates as follows:

- Get assigned input parameters related to the type of radar being simulated and the bioscatterers to be observed (discussed below and in Tables 1 and 2).
- Based on the input parameters and for each assigned value of range r_o, create a one-way beam weighting function $f^2(\theta, \phi)$ (Eq. 2) and one-way range weighting function $W(r)$ (Eq. 3).
- Using the weighting function, define a radar sampling volume (Eq. 6).
- Create a domain within the simulator based on the radar sampling volume. Whereas the radar sampling volume theoretically extends over all space, bioscatterers located far from its center are not expected to contribute appreciably to the collective bioscatter. The simulator domain is defined such that it encompasses values of r, θ, and ϕ large enough to allow $f^4(\theta, \phi)$ and $W^2(r)$ to achieve values of -12 dB or greater.
- Randomly populate the simulator domain with bioscatterers consistent with a specified number density N_{bio} and assign each with a radar cross section. The same value of σ is used for all bioscatterers.
- Calculate the backscattered power from the

Table 1. Typical technical specifications for the WSR-88D.

Parameter	Value	Unit
Antenna diameter	8.53	m
Beam width (3-dB, one-way)	0.96	deg
Antenna gain	45	dB
Wavelength	10.7	cm
Transmit power	1000	kW
Pulse width	1.57	μs
Receiver bandwidth	0.63	MHz
Minimum detectable signal	−113	dBm
Range gate spacing	250	m

Note: Parameters used in the simulation are indicated in bold.

sum of the range- and beam-weighted contributions from all bioscatterers within the simulator domain (Eq. 5).

- Calculate radar reflectivity (Eq. 12) and effective radar reflectivity factor (Eq. 17).

The radar simulator as a whole is designed to call the primary scattering routine repeatedly with different values of r_o and N_{bio}. An ensemble of samples is generated by running the simulator repeatedly using the sample input parameters. The only aspect of the simulator that changes in this case is the randomly assigned locations of the bioscatterers.

Simulator setup and implementation

The simulator was configured according to the technical specifications for one of the WSR-88Ds that make up the NEXRAD network. A partial listing of the technical specifications of a WSR-88D is provided in Table 1. Parameters used in the simulation are indicated in bold. The simulator developed for this study focuses on the distribution and number density of the bioscatterers. It does not include the effects of system noise, interference, or other factors that limit the bioscatter detectability. If this were the case then the gain, transmit power, bandwidth, and minimum detectable signal would need to be considered. More information on the WSR-88Ds and NEXRAD can be found in (Doviak and Zrnić 1993, Committee on Weather Radar Technology Beyond NEXRAD 2002, Rinehart 2004).

Having established the radar specifications, we now consider parameters used by the simulator that describe operation of the radar, the bioscatterers, and ensemble averaging. These values are summarized in Table 2. Weather radars typically scan the environment using several settings for the antenna elevation angle. Since most bioscatterers are located near the Earth's surface, we are only simulating an elevation angle of 0.5°, which is a common value for the lowest elevation scan for NEXRAD. As discussed above, the simulator steps through a series of values of range r_o. The values used to initiate the loops to generate r_o for the present study are provided in Table 2. The combination of the antenna elevation angle and range is used to determine the height above ground of the sampling volume.

Table 2. Parameters used in the radar simulator.

Parameter	Value	Unit
Antenna elevation angle	0.5	deg
Minimum range	10	km
Maximum range	200	km
Range step size	5	km
Minimum number density	50	$1/km^3$
Maximum number density	250	$1/km^3$
Number density step size	50	$1/km^3$
Radar cross section	10	cm^2
Number of simulated realizations	5000	...

When calculating the height of the radar beam above the Earth's surface, the 4/3 Earth radius model was used (Doviak and Zrnić 1984). This model takes into account the effects of refraction based on a standard model of the Earth's atmosphere. Shown in the upper panel of Fig. 2 is a depiction of the beam geometry for a WSR-88D scanning at a 0.5° elevation angle. The upper and lower bounds for the beam are based on the 3-dB beam width of the radar. See Table 1.

We next consider those parameters used to control the bioscatterers and the ensemble averaging. As for the range r_o, the simulator steps through a series of values of the bioscatter number density N_{bio}. Values of N_{bio} are given in terms of the number of bioscatterers contained within a one cubic kilometer volume. That is, $N_{bio} = 100/km^3$ designates 100 animals per cubic kilometer. From N_{bio} we can then calculate the number of bioscatterers within a radar sampling volume using

$$n_{bio} = N_{bio} V_{rad}. \quad (21)$$

In the lower panel of Fig. 2 we show n_{bio} as a function of range for various assumed number

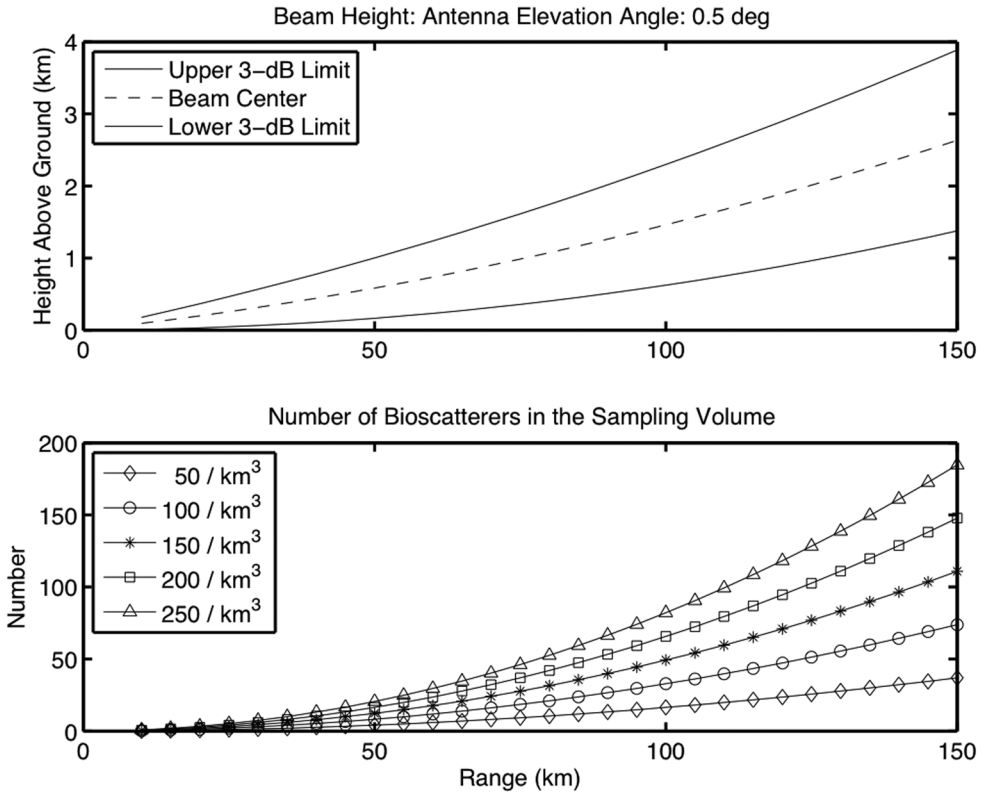

Fig. 2. Upper panel: Vertical cross-section of the radar beam at an elevation angle of 0.5° calculated using the 4/3 Earth radius model. The displacement from the lower to upper edge of the sampling domain for a given range r_o as defined by the 3-dB beam width is given by $r_o\phi$. See Fig. 1. Lower panel: Number of bioscatterers contained in a radar sampling volume as a function of range. Curves for five different assumed number densities of bioscatterers are shown. Values of N_{bio} are given as bioscatterers per cubic kilometer. That is, 50 bioscatterers per cubic kilometer is 50/km^3. These calculations are valid for NEXRAD and for a transmitted pulse width of 1.57 μs.

densities. The plot corresponds to the specifications for a WSR-88D with a pulse width of 1.57 μs. The selected values of N_{bio} are representative of migrating or foraging birds and bats (Bruderer 1999, Dokter et al. 2011). Much larger values would be needed to represent number densities for insects or during some emergences of roosting birds or bats.

For the present analysis, a single value of σ is used for all calculations and it is assumed that σ has no angular dependence. Representative RCS values for birds reported in the literature include $\sigma = 11$ cm^2 (Dokter et al. 2011) and $\sigma = 15$ cm^2 (Diehl et al. 2003). Here we use $\sigma = 10$ cm^2, which represents a small passerine songbird or bat. The simulator was run 5000 times for each realization of the different ranges and number densities shown in Table 2 to create an ensemble of results for statistical calculations. For each individual realization of the Monte-Carlo type simulation described we present means and standard deviations calculated for both the radar reflectivity (Eq. 12) and effective radar reflectivity factor (Eq. 17).

Effects of non-uniform distribution of bioscatter

We briefly consider the case of non-uniformly distributed bioscatterers in the aerosphere and how non-uniformity might impact our simulation and interpretation of radar reflectivity. Whereas it may be safe to assume that bioscatterers are uniformly distributed horizontally within the domain of a radar sampling volume, this is less likely to be the case along the vertical

extent. Clearly the number of animals in the aerosphere must decrease with height. Moreover, their distribution in height can vary depending on wind conditions, time of year, location, and so forth (Bruderer and Liechti 1998, Dolbeer 2006, Schmaljohan et al. 2008, Bruderer et al. 2008, Buler and Diehl 2009, Dokter et al. 2011). Therefore N_{bio} should ideally be treated as a function of height. However, it is neither feasible nor possible in the present study to fully account for the wide range of height variability in N_{bio}. As an alternative, we present a means of partly accounting for this height dependence.

Let us reconsider the effective radar sampling volume. Earlier we showed that the radar sampling volume is tapered in space as a result of the beam and range weighting functions through Eqs. 2 and 3, respectively. For the sake of mathematical expediency, let the combined effects of these functions be expressed in Cartesian coordinates as a one-way, three-dimensional volume weighting function $W_{vol}(x, y, z)$ such that

$$V_{rad} = \int_{-\infty}^{\infty}\int_{-\infty}^{\infty}\int_{-\infty}^{\infty} W_{vol}^2(x,y,z)dxdydz. \quad (22)$$

This is equivalent to Eq. 6. As before, $n_{bio} = N_{bio}V_{rad}$ provided N_{bio} is uniformly distributed and the volume-filling assumption applies. If N_{bio} is not uniformly distributed in height then the effective number of bioscatterers contained within a radar sampling volume can be expressed as

$$n_{bio} = \int_{-\infty}^{\infty}\int_{-\infty}^{\infty}\int_{-\infty}^{\infty} W_{vol}^2(x,y,z)N_{bio}(z)dxdydz \quad (23)$$

where $N_{bio}(z)$ is now written explicitly as a function of height (z).

To account for the height dependence of N_{bio} we can assume that the distribution of bioscatterers in the aerosphere can be modeled using a normalized probability distribution function (pdf) $p(z)$ such that $N_{bio}(z) = N_o p(z)$, where N_o is a scaling factor. The quantity N_o has units of N_{bio} and can be adjusted to reflect temporal variations in the bioscatter. Using this convention, we can write

$$\begin{aligned} n_{bio} &= N_o\int_{-\infty}^{\infty}\int_{-\infty}^{\infty}\int_{-\infty}^{\infty} W_{vol}^2(x,y,z)p(z)dxdydz \\ &= N_o V'_{rad} \end{aligned} \quad (24)$$

where

$$V'_{rad} = \int_{-\infty}^{\infty}\int_{-\infty}^{\infty}\int_{-\infty}^{\infty} W_{vol}^2(x,y,z)p(z)dxdydz. \quad (25)$$

That is, using Eqs. 24 and 25 we can treat the number density of bioscatterers as a 'constant' and account for the height dependence by modifying the effective radar sampling volume.

As an example, consider a collection of bioscatterers that are log-normally distributed in height. In this case the pdf is expressed as

$$p(z) = \frac{1}{z\sqrt{2\pi\sigma^2}}\exp\left[-\frac{(\ln z - \mu)^2}{2\sigma^2}\right] \quad (26)$$

where μ and σ are the mean and standard deviation of the underlying normal distribution, respectively. Using values $N_o = 100000/km^3$, $\sigma = 0.8$, and $\mu = 6.34$ for the pdf shown in Eq. 26 and a uniform distribution along the horizontal extent, we have generated locations of bioscatters within a 1 km × 1 km × 1 km box. This can be seen in Fig. 3. The chosen value of N_o corresponds to a vertically integrated value of 100 bioscatterers per km^2 and the values of μ and σ result in a mode of 300 m for the pdf. These values were motivated in part by the results shown in Fig. 3 of Dokter et al. (2011). For reference, we show upper and lower bounds of the two-way beam pattern for NEXRAD (defined by the 3-dB points) that would result using a 0.5° elevation angle and assuming that the center of the box is located 50 km and 100 km from the radar.

When deriving the proposed method to account for $N_{bio}(z)$ it has been implicitly assumed that the volume filling assumption applies. As we have already discussed, when that assumption breaks down, a degree of uncertainty is introduced into our estimates of radar reflectivity. It should be noted that there is a distinct difference between the actual weighting functions used for the radar sampling volume and the proposed weighting function to account for $N_{bio}(z)$. Bioscatterers further from the center of the radar sampling volume will actually contribute less to the collective received power by the radar. They are being illuminated with less power from the radar and the radar is less sensitive to the power they reflect. However, for the case of $N_{bio}(z)$, the actual numbers of animals

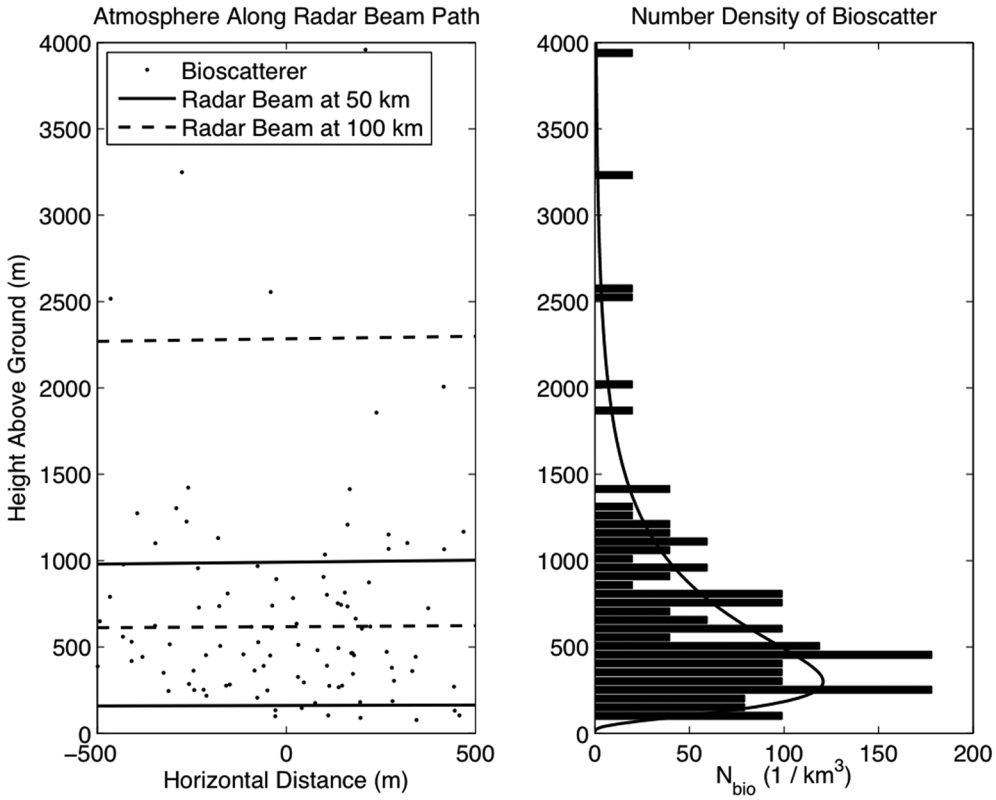

Fig. 3. Left panel: A depiction of the positions of bioscatterers with an assumed uniform distribution in space horizontally and a log-normal distribution in height. Also shown are the upper and lower bounds of a radar beam for a radar located at 50 and 100 km away. Right panel: A histogram height dependence in bioscatter number density for the case shown in the left panel. The bin sizes in the histogram are 20 m. The assumed pdf (sampled at 1-m intervals) is shown for comparison.

are decreasing with height. We are simply approximating the effect by shaping the sampling volume with a height-dependent weighting function given by the pdf. The more scatterers in the sampling volume, the better the approximation becomes.

Results

Results of the study show that estimated mean values of η calculated for all ranges from the radar approach the expected values used in the simulation, demonstrating the feasibility of using mean η to estimate animal densities. However, the variance of the estimates exhibits a notable range dependence. A range dependence is anticipated since the radar sampling volume increases with increasing distance from the radar and we have assumed a constant number density of bioscatterers in the simulation. This effect is illustrated in Fig. 4 by plotting the mean, median, and confidence interval (CI) of the mean from our estimates of the radar reflectivity obtained from the simulator. The expected value of radar reflectivity in this case is 1000 cm^2/km^3. Since number density of bioscatterers is fixed, sampling volumes at greater ranges encompass a larger number of bioscatterers. Consequently, the likelihood of the volume-filling assumption being fulfilled for a given range improves and the standard deviation of the estimate of reflectivity decreases. Keep in mind that N_{bio} is being held constant. To account for a potential decrease N_{bio} with height, one could use Eq. 24 to adjust the effective size of the radar sampling volume.

Note that the confidence intervals shown in Fig. 4 become increasingly asymmetric about the mean with decreasing range from the radar.

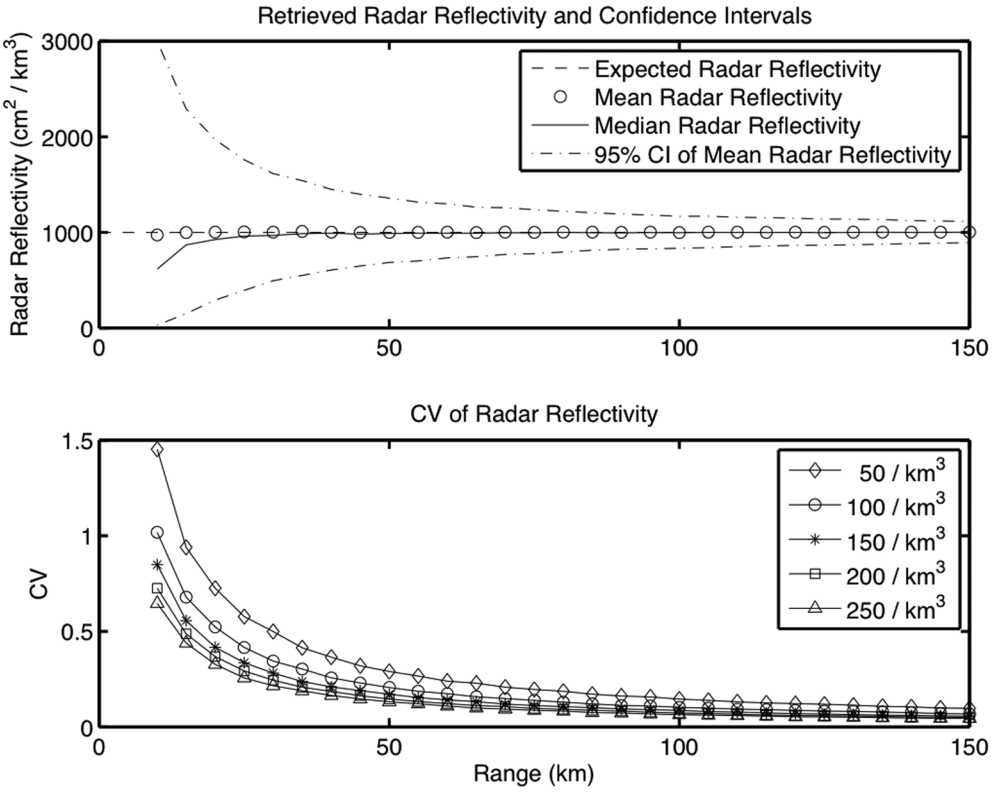

Fig. 4. Upper panel: Estimates of the mean, median, and confidence interval of the mean for observed radar reflectivity using an assumed number density of $N_{bio} = 100/km^3$ and RCS of $\sigma = 10$ cm^2. Lower panel: Coefficient of variation of the radar reflectivity estimates for different values of the number density of bioscatterers. Both plots were calculated using the parameters provided in Table 1.

Moreover, the median of the estimated radar reflectivity correspondingly decreases. These effects are indicative of a transition from having a few discrete bioscatterers within a radar sampling volume to the case of distributed (and possibly volume-filling) bioscatterers. In the former case, Eq. 5 should be applied, which predicts that the received power exhibits a $1/r^4$ dependence in range. For distributed bioscatterers, we expect a $1/r^2$ dependence as indicated in Eq. 12. Therefore when the number of bioscatterers is small, estimates of radar reflectivity will be biased low for most samples (decreasing median); however, some of the samples will result in an overestimation of η, e.g., if a single bioscatterer is located at or near the center of the radar sampling volume. As the number of bioscatterers in a sampling volume increases, estimates of the median approach the mean and the confidence intervals become more symmetric about the mean, which can be interpreted as a measure of the degree to which the volume-filling assumption is fulfilled. For the case shown in Fig. 4, this appears to occur at a range of about 50 km.

The validity of the volume-filling assumption and our ability to accurately estimate radar reflectivity is ultimately related to the number of bioscatterers present within a given radar sampling volume, which is affected by both the size of the sampling volume and the number density of bioscatterers. We have shown that the standard deviation in our estimates of radar reflectivity increases as the radar sampling volume decreases, resulting in a break down of the volume-filling assumption. However, what happens when the number density of bioscatterers increases? For a given sampling volume, this condition should increase the likelihood of meeting the volume-filling assumption. Howev-

er, the value of η increases with an increase in the number density (Eq. 13), which also leads to an increase in the standard deviation. Therefore, we use the coefficient of variation (CV; standard deviation divided by the mean) of η when exploring the impacts of sampling volume size and number density on the uncertainty of our radar reflectivity estimates. A plot of the CV of η as a function of range and number density is provided in the lower panel of Fig. 4. The CV decreases both for increasing range and increasing number density.

The results presented in Fig. 4 are valid for NEXRAD; however, we would like to generalize the analysis for other weather radar systems. To this end, we consider how CV of η varies in response to the number of bioscatterers per sampling volume (Eq. 21). For each of the data points shown in the lower panel of Fig. 4, we calculated a value of n_{bio}. A linear relationship emerges when $\log_{10}(\text{CV of } \eta)$ is plotted versus $\log_{10}(n\text{bio})$ as shown in the upper panel of Fig. 5. When fitted using a linear regression algorithm, we find that

$$\text{CV of } \eta = 0.59 n_{\text{bio}}^{-0.5}. \quad (27)$$

This result should be general according to the mathematical treatment provided above. Moreover, since η and N_{bio} are linearly related through σ (Eq. 13), if σ is constant, then we can use Eq. 27 to calculate the STD of N_{bio}.

Based on the antenna characteristics and operating parameters of a particular radar, the number of bioscatterers per sampling volume n_{bio} can easily be found for different assumed values of the animal number density N_{bio} using Eq. 10 together with Eq. 21. An example of such calculations for NEXRAD is shown in the lower panel of Fig. 5. Having estimated n_{bio}, Eq. 27 can then used to find the corresponding value of CV for η. Although N_{bio} is not known from the radar observations alone, it can be estimated using the calculated value of η and using an assumed value of σ.

Discussion

Past efforts to quantify aerial densities based on radar observations have typically relied on comparing relative values of Z (Horn and Kunz 2008, Buler and Moore 2011) or used linear regression to calibrate densities estimated from individual bioscatterers from marine radar to reported values of Z from NEXRAD installations (Diehl et al. 2003, van Gasteren et al. 2008, Buler and Diehl 2009). While these efforts have proved useful for answering ecological questions in certain contexts (Russell et al. 1998, Bonter et al. 2009), they have limited generality and rely on the radar reflectivity factor, which assumes properties inherent to meteorological entities. Using a 'first principles' approach, we show that η relates more directly to biologically derived radar signal and therefore should be used as the basis for interpreting densities of biological entities from radar signals in future efforts. Transformation from Z to η is easily accomplished (Eq. 19) and should not impede future efforts. We demonstrate the mathematics of interpreting received echo power in terms of density of bioscatterers and examine the relationships among measurement error and these bioscatter signals. We also present a framework for using radar echoes for quantifying biological populations observed by radar in their aerosphere habitats. We argue that this framework will enhance use of radar remote-sensing for long-term population monitoring as well as a host of other ecological applications, such as studies on phenology, movement, and aerial behaviors. Advances in radar aeroecology will be facilitated by a solid understanding of the radar equation in its different forms and the various assumptions involved when deriving them.

One of the limitations of using radar data for quantifying population densities and its subsequent ability for long-term population monitoring is lack of sufficient understanding of the measurement error associated with reported reflectivity values for a given radar sampling volume and how that measurement error is related to the number of scatterers within a given volume at different ranges from a radar (Horn and Kunz 2008). While these relationships have been considered in detail for meteorological scatter, how such radar theory applies to biological entities is in its nascency. Typically, the radar equation is applied to one of two cases: echo power comes from a single entity or echo power is from a large collection of entities for which the volume-filling assumption is valid. For

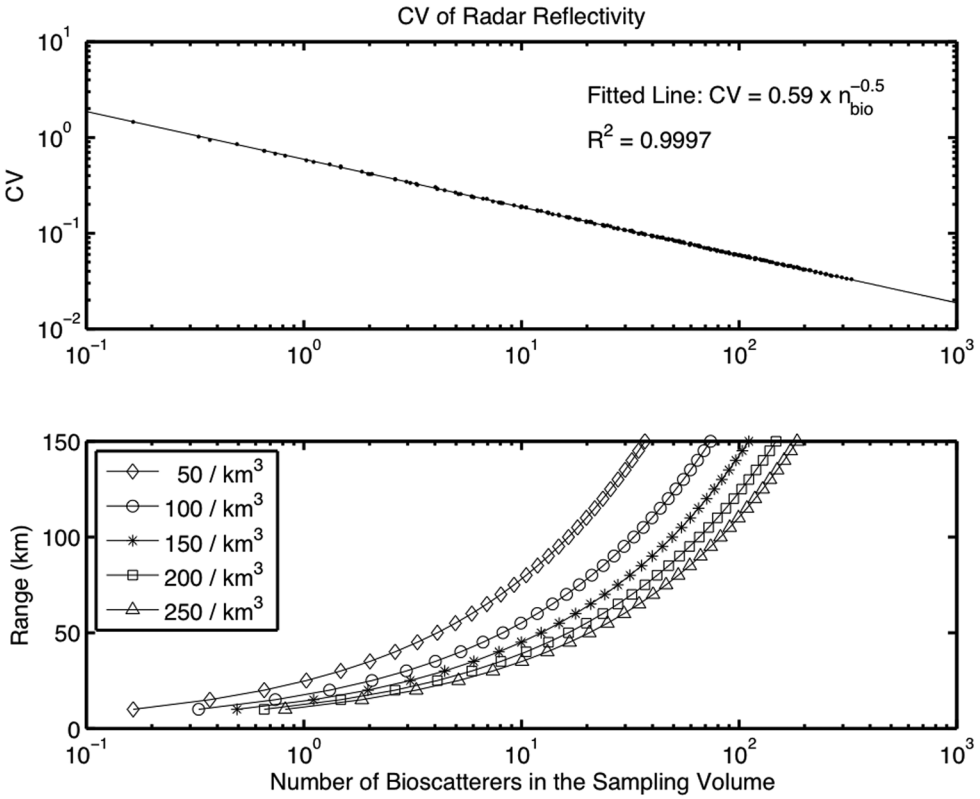

Fig. 5. Upper panel: Coefficient of variation of the radar reflectivity estimates for different values of the number density of bioscatterers shown with the resulting fitted line given by Eq. 27. The coefficient of determination for the fit is given as R^2. Lower panel: Reference plot valid for NEXRAD to be used when interpreting the result shown in the upper panel.

the case of bioscatter, neither of these conditions may apply, making an interpretation of echo power difficult. A confounding measurement error arises from uncertainties in the RCS values of the animals observed. One does not typically know a priori the type of animal present. Moreover, shape and orientation affects the RCS of a biological entity. In the present treatment we have not considered these effects.

We have shown that estimates of radar reflectivity will inherently contain a certain amount of error whenever the volume-filling assumption does not apply. When volume-filling does apply, measurement error decreases with increased densities and range from a radar (Fig. 2). These results provide the first attempt at a general framework for understanding how to compare relative values of radar reflectivity that represent signal received from numbers of animals aloft. By explicitly accounting for error and knowing the effects of range and density on measurement error, radar data can be converted to number densities of animal populations with known precision, which permits use for comparative studies and long-term monitoring of populations regularly observed with radar, e.g., Brazilian free-tailed bat (*Tadarida brasiliensis*) or purple martin (*Progne subis*) colonies (Horn and Kunz 2008, Kelly et al. 2012).

Based on results from our Monte-Carlo based radar simulator, we have been able to show how error estimates of radar reflectivity are impacted when certain assumptions used to calculate η are not valid. By introducing the coefficient of variation of η, we relate the expected variance in η to the number of bioscatterers n_{bio} present within a given radar sampling volume, which provides a basis for developing unbiased estimators for measuring the number of animals aloft from radar observations. Estimates of n_{bio}

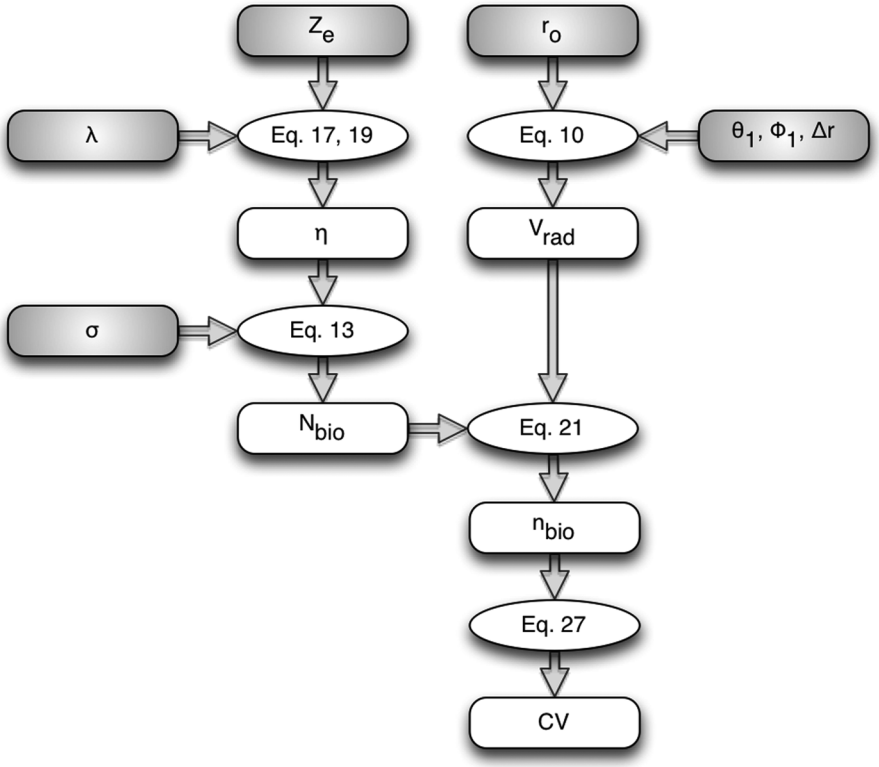

Fig. 6. Diagram illustrating the workflow for calculating biologically relevant parameters from radar products, where Z_e is the equivalent radar reflectivity factor reported from NEXRAD, λ is radar wavelength (e.g., 10 cm for a S-band NEXRAD radar), σ is the RCS for a given organism, r_o is the range (distance) from the radar, θ_1 , ϕ_1 and Δr are the horizontal and vertical the one-way half-power beamwidths and range resolution, respectively, η is radar reflectivity, N_{bio} is the number of bioscatterers per unit volume, V_{rad} is the radar sampling volume, n_{bio} is the number of bioscatterers per radar sampling volume, and CV is the coefficient of variation associated with an estimate of n_{bio}.

can be found in turn for a particular set of measurements if the radar sampling volume V_{rad} and the number of density of animals N_{bio} are known. The former can be calculated if certain specifications of the radar and how it was operated are known, which is generally the case for most radars. The latter can be estimated using observed values of η if one can assume a representative value of σ for the observations. Alternatively, one might use a representative value of N_{bio} for the particular biological phenomena being observed. In Fig. 6, we demonstrate how calculations described in this paper can be used to derive biologically meaningful estimates of number densities of aerial organisms directly from radar products if associated parameters such as the RCS of an organism are known.

The practical applications of our results are best demonstrated through a biological example. Brazilian free-tailed bats form large maternity aggregations in caves throughout the American southwest during the summer, which are easily observable on NEXRAD. Two large colonies readily detected by NEXRAD when bats emerge in the evening are Bracken and Frio Caves in southern Texas. Frio Cave is located approximately 60 km from a WSR-88D site (KDFX) and Bracken is 31 km from another WSR-88D site (KEWX). To illustrate effects of range on CVs, assume that bats emerge from both caves with equal number densities ($N_{bio} = 300/km^3$) that are uniformly distributed in space. At Bracken Cave we expect 9.5 bats per sampling volume, which

corresponds to CV of $\eta = 0.19$ (Eq. 27). At Frio Cave the expected number of bats per sampling volume is 35 and CV of $\eta = 0.10$. Therefore, estimates of population sizes based on radar reflectivity at Frio Cave will be more precise than those at Bracken Cave because of this range effect. However, proximity to a radar station confers an advantage in that most biological activity in the aerosphere occurs at lower altitudes. At sites that are much greater than 90 km from a NEXRAD station, biological entities are typically flying quite literally "under the radar" and therefore estimates of population size may be biased by limited detectability based on beam height (Fig. 2).

In summary, we contend that radar reflectivity is a more meaningful measure of echo power than the equivalent radar reflectivity factor reported by weather radars when considering bioscatter. There are clear advantages of working with weather radar data for aeroecological studies. In addition to providing continuous data streams with wide spatial coverage, users benefit from the efforts of the weather services to maintain and calibrate the radars and preprocess the received echo powers. This preprocessing involves (1) calculating and removing noise from the echo signal, (2) correcting the power to account for range squared effects, (3) calculating each sampling volume V_{rad}, and finally (4) calculating the effective radar reflectivity factor Z_e. However, we have shown how η expressed in dB can be easily related to Z_e expressed in dBZ (Eq. 19). To that end, it may be worthwhile to consider a new dB value that specifically applies to bioscatter. There are many examples of dB values that have special designators such as those for the radar reflectivity factor relative to 1 mm^6/m^3 (dBZ), RCS relative to one square meter (dBsm), power relative to one mW (dBm or dBmW), gain of an antenna relative an isotropic antenna (dBi), and so forth. Perhaps an appropriate decibel unit of radar reflectivity from bioscatter relative to 1 cm^2/km^3 would be the dBη.

As we continue to draw upon weather radar data for the study of animal movements in the aerosphere and use them to derive useful and quantifiable biological parameters, it becomes incumbent upon us to draw inspiration from classic literature and ponder for a moment the age-old message:

To Z or not to Z? That is the question:
Whether 'tis nobler in the mind to suffer
The slings and arrows of outrageous assumptions
Or to take arms against a sea of inappropriate nomenclature
And by opposing end them.

When dealing with and interpreting weather radar data for quantitative biological studies, we feel that the answer to this question is clear: it is better *not to Z*.

Acknowledgments

PBC and PMS were supported through internal funding from the University of Oklahoma. JFK and JRS were supported by NSF Grants IOS-0541740 and EPS-0919466. WFF was supported by NSF DBI-0905881.

Literature Cited

Alerstam, T. 1990. Bird migration. Cambridge University Press, Cambridge, UK.

Alerstam, T., J. W. Chapman, J. Bäckman, A. D. Smith, H. Karlsson, C. Nilsson, D. R. Reynolds, R. H. G. Klaassen, and J. K. Hill. 2011. Convergent patterns of long- distance nocturnal migration in noctuid moths and passerine birds. Proceedings of the Royal Society B 278:3074–3080.

Battan, L. J. 1973. Radar observations of the atmosphere. University of Chicago Press, Chicago, Illinois, USA.

Bonter, D. N., S. A. Gauthreaux, Jr., and T. M. Donovan. 2009. Characteristics of important stopover locations for migrating birds: Remote sensing with radar in the Great Lakes basin. Conservation Biology 23:440–448.

Bruderer, B. 1997*a*. The study of bird migration by radar. Part 1: The technical basis. Naturwissenschaften 84:1–8.

Bruderer, B. 1997*b*. The study of bird migration by radar. Part 2: Major achievements. Naturwissenschaften 84:45–54.

Bruderer, B. 1999. Three decades of tracking radar studies on bird migration in Europe and the Middle East. Pages 107–142 *in* Y. Leshem, Y. Mandelik, and J. Shamoun-Baranes, editors. Proceedings of the International Seminar on Birds and Flight Safety in the Middle East. Tel Aviv University, Tel Aviv, Israel.

Bruderer, B., and F. Liechti. 1998. Flight behaviour of nocturnally migrating birds in coastal areas: crossing or coasting. Journal of Avian Biology 29:499–507.

Bruderer, B., D. Peter, and T. Steuri. 1999. Behaviour of

migrating birds exposed to X-band radar and a bright light beam. Journal of Experimental Biology 202:1015–1022.

Bruderer, B., L. G. Underhill, and F. Liechti. 2008. Altitude choice by night migrants in a desert area predicted by meteorological factors. Ibis 137:44–45.

Buler, J. J., and R. H. Diehl. 2009. Quantifying bird density during migratory stopover using weather surveillance radar. IEEE Transactions on Geoscience and Remote Sensing 47:2741–2751.

Buler, J. J., and F. R. Moore. 2011. Migrant-habitat relationships during stopover along an ecological barrier: extrinsic constraints and conservation implications. Journal of Ornithology 152:101–112.

Chapman, J. W., V. A. Drake, and D. R. Reynolds. 2011. Recent insights from radar studies of insect flight. Annual Review of Entomology 56:337–356.

Chilson, P. B., W. F. Frick, J. F. Kelly, K. W. Howard, R. P. Larkin, R. H. Diehl, J. K. Westrook, T. A. Kelly, and T. H. Kunz. 2012. Partly cloudy with a chance of migration: Weather, radars, and aeroecology. Bulletin of the American Meteorological Society 93:669–686.

Committee on Weather Radar Technology Beyond NEXRAD. 2002. Weather radar technology beyond NEXRAD. National Academies Press, Washington, D.C., USA.

Crum, T., R. Saffle, and J. Wilson. 1998. An update on the NEXRAD program future WSR-88D support to operations. Weather and Forecasting 13:253–262.

Diehl, R. H., and R. P. Larkin. 2005. Introduction to the WSR-88D (NEXRAD) for ornithological research. Technical Report PSW-GTR-191. USDA Forest Service.

Diehl, R. H., R. P. Larkin, and J. E. Black. 2003. Radar observations of bird migration over the Great Lakes. Auk 120:278–290.

Dokter, A. M., F. Liechti, H. Stark, L. Delobbe, P. Tabary, and I. Holleman. 2011. Bird migration flight altitudes studied by a network of operational weather radars. Journal of Royal Society Interface 8:30–43.

Dolbeer, R. A. 2006. Height distribution of birds recorded by collisions with civil aircraft. Journal of Wildlife Management 70:1345–1350.

Doviak, R., and D. S. Zrnić. 1984. Reflection and scatter formula for anisotropically turbulent air. Radio Science 19:325–336.

Doviak, R. J., and D. S. Zrnić. 1993. Doppler radar and weather observations. Second edition. Dover, New York, New York, USA.

Eastwood, E. 1967. Radar ornithology. Methuen, London, UK.

Eckhardt, R. 1987. Stan Ulman, John von Neumann, and the Monte Carlo method. Los Alamos Science 15:131–137.

Gauthreaux, S. A., Jr. 1970. Weather radar quantification of bird migration. BioScience 20:17–20.

Gauthreaux, S. A., Jr. 2006. Bird migration: Methodologies and major research trajectories (1945–1995). Condor 98:442–453.

Gauthreaux, S. A., Jr., and C. G. Belser. 1998. Displays of bird movements on the WSR-88D: Patterns and quantification. Weather and Forecasting 13:453–464.

Gauthreaux, S. A., Jr., and C. G. Belser. 2003. Bird movements on Doppler weather surveillance radar. Birding 35:616–628.

Gauthreaux, S. A., Jr., J. W. Livingston, and C. G. Belser. 2008. Detection and discrimination of fauna in the aerosphere using Doppler weather surveillance radar. Integrative and Comparative Biology 48:12–23.

Harmata, A. R., G. R. Leighty, and E. L. O'Neil. 2003. A vehicle-mounted radar for dual-purpose monitoring of birds. Wildlife Society Bulletin 31:882–886.

Horn, J. W., and T. H. Kunz. 2008. Analyzing NEXRAD Doppler radar images to assess nightly dispersal patterns and population trends in Brazilian free-tailed bats (*Tadarida brasiliensis*). Integrative and Comparative Biology 48:24–39.

Kelleher, K. E., K. K. Droegemeier, J. J. Levitt, C. Sinclair, D. E. Jahn, S. D. Hill, L. Mueller, G. Qualley, T. D. Crum, S. D. Smith, S. A. D. Greco, S. Lakshmivarahan, L. Miller, M. Ramamurthy, B. Domenico, and D. W. Fulker. 2007. Project CRAFT: A real-time delivery system for NEXRAD level II data via the internet. Bulletin of the American Meteorological Society 88:1045–1057.

Kelly, J. F., J. R. Shipley, P. B. Chilson, K. W. Howard, W. F. Frick, and T. H. Kunz. 2012. Quantifying animal phenology in the aerosphere at a continental scale using NEXRAD weather radars. Ecosphere 3:16.

Kunz, T. H., S. A. Gauthreaux, Jr., N. I. Hristov, J. W. Horn, G. Jones, E. K. V. Kalko, R. P. Larkin, G. F. McCracken, S. M. Swartz, R. B. Srygley, R. Dudley, J. K. Westbrook, and M. Wikelski. 2008. Aeroecology: probing and modeling the aerosphere. Integrative and Comparative Biology 48:1–11.

Larkin, R. P., and R. H. Diehl. 2012. Radar techniques for wildlife biology. Pages 319–335 *in* N. Silvy, editor. The wildlife techniques manual: research. Volume 1. Seventh edition. Wildlife Society, Baltimore, Maryland, USA.

Liechti, F., B. Bruderer, and H. Paproth. 1995. Quantification of nocturnal bird migration by moonwatching: comparison with radar and infrared observations. Journal of Field Ornithology 66:457–652.

Martin, W. J., and A. Shapiro. 2007. Discrimination of bird and insect radar echoes in clear air using high-resolution radars. Journal of Atmospheric and Oceanic Technology 24:1215–1230.

Mie, G. 1908. Beitraäge zur Optik trüber Medien, speziell kolloidaler Metallősungen. Annalen der Physik 25:377–445.

Nebuloni, R., C. Capsoni, and V. Vigorita. 2008. Quantifying bird migration by a high-resolution weather radar. IEEE Transactions on Geoscience and Remote Sensing 46:1867–1875.

Probert-Jones, J. R. 1962. The radar equation in meteorology. Quarterly Journal of the Royal Meteorological Society 88:485–495.

Rinehart, R. E. 2004. Radar for meteorologists. Fourth edition. Rinehart, Columbia, Missouri, USA.

Russell, K. R., and S. A. Gauthreaux, Jr. 1998. Use of weather radar to characterize movements of roosting purple martins. Wildlife Society Bulletin 26:5–16.

Russell, K. R., D. S. Mizrahi, and S. A. Gauthreaux, Jr. 1998. Large-scale mapping of purple martin premigratory roosts using WSR-88D weather surveillance radar. Journal of Field Ornithology 69:316–325.

Sauvageot, H. 1992. Radar meteorology. Artech House, Boston, Massachusetts, USA.

Schmaljohan, H., F. Liechti, E. Bächler, T. Steuri, and B. Bruderer. 2008. Quantification of bird migration by radar—a detection probability problem. Ibis 150:342–355.

Serafin, R. J., and J. W. Wilson. 2000. Operational weather radar in the United States: Progress and opportunity. Bulletin of the American Meteorological Society 81:501–518.

Shamoun-Baranes, J., A. M. Dokter, H. van Gasteren, E. E. van Loon, H. Leijnse, and W. Bouten. 2011. Birds flee en mass from New Year's Eve fireworks. Behavioral Ecology 22:1173–1177.

van Gasteren, H., I. Holleman, W. Bouten, E. van Loon, and J. Shamoun-Baranes. 2008. Extracting bird migration information from C-band Doppler weather radars. Ibis 150:674–68.